Sensitivity of Predicted Temperature in a Fillet Weld T-Joint to Parameters Used in Welding Simulation with Prescribed Temperature Approach

Kien Nguyen[1], Reza Nasouri[2], Caroline Bennett[1], Adolfo Matamoros[2], Jian Li[1], Arturo Montoya[2]

[1] Department of Civil, Environmental and Architectural Engineering, University of Kansas

[2] Department of Civil and Environmental Engineering, University of Texas at San Antonio

Abstract: Abaqus can be used to simulate welding processes, but the procedure can be time consuming due to a large number of steps necessary to generate weld beads and the associated thermal loads and convective film interactions. Recent development of the Abaqus Welding Interface (AWI) addresses these challenges, as the AWI utility automatically creates all of those steps. While the AWI procedure is quite straightforward, its accuracy can be expected to be highly dependent on the magnitude of several parameters defined in AWI: torch temperature, temperature ramping option, and deposited weld "chunk" length. To use the AWI capabilities, these parameters need to be calibrated to achieve a proper thermal solution for each welding simulation. However, there is no available guidance on the calibration procedure, and the effects of these parameters are not fully understood. This paper presents a sensitivity study of temperature fields to these parameters using a case study of a T-joint fillet weld. Ten models were created in which the welding process was simulated using the AWI utility with varying torch temperatures, ramping options, and deposited weld chunk. The obtained results were compared with available data from published work for the same welded detail. For the weld studied, it was observed that the best option for the weld chunk size was 10mm, while the torch temperature should be in the range of 1400-1500°C, which can be complemented by adjusting the ramping options to obtain an improved result. A discussion regarding a general procedure using the AWI to calibrate a welding simulation, and the merits of the prescribed temperature approach used in AWI is presented.

1. Introduction

Using the finite element method to simulate a welding process can require significant effort. A large number of modeling steps often must be created to capture geometric features, multiple weld passes, material properties, and thermal and structural boundary conditions. Recent development of the Abaqus Welding Interface (AWI) addresses these challenges, as the AWI utility automatically creates all of those steps (Shubert et al., 2010).

Generally, two approaches have been used to capture the effects of the welding heat source in finite element simulations: *prescribed temperature* and *prescribed heat input* (Goldak & Akhlaghi, 2005; Lindgren, 2001). The former approach has been widely used, especially in the

1990s and 2000s. It was used to simulate single-pass welds in work performed by (Carmet et al., 1988; Goldak et al., 1996; Jones et al., 1993a, 1993b; Lindgren, 2006). It was also utilized to simulate multi-pass welds in (Lindgren et al., 1999; Roelens, 1995a, 1995b; Roelens et al., 1994). In this approach, the prescribed temperature has generally been defined as the liquidus temperature (having a higher magnitude than the melting temperature). In the AWI, the prescribed temperature approach has been used since its release in 2012. A new option of using the prescribed heat input approach with the Goldak double ellipsoid (Goldak et al., 1984) will be introduced in the AWI in 2017. The study in this paper used the available prescribed temperature approach that is employed by the AWI utility.

When the AWI with the prescribed temperature approach is used, welding is simulated using a sequential thermal-mechanical analysis, in which a heat transfer analysis is performed to generate a temperature history by applying a prescribed temperature (called the *torch temperature* in the AWI) at the boundary between the current weld pass and the neighboring region (base material or already deposited weld pass). The applied temperature is required to be ramped over a period of time, over which a certain length of weld metal (called a *weld chunk* in the AWI) is deposited into the weld pool. In the AWI, the deposited weld chunk is not directly defined, but is controlled through the definition of the *Time Period* in the "Pass Step Control 3D" window, as shown in Figure 1. An illustration of the prescribed temperature approach is presented in Figure 2.
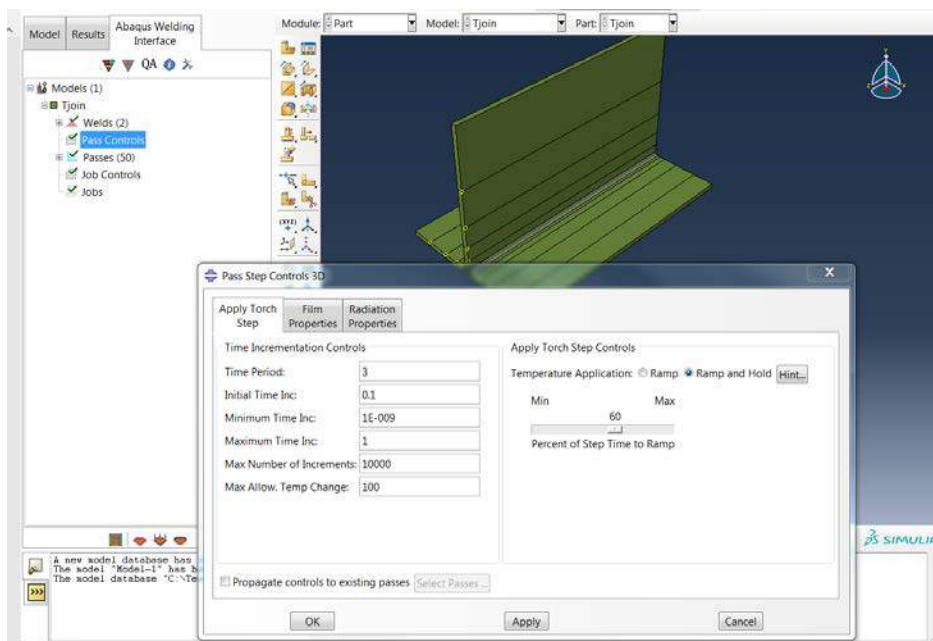

Figure 1. Creation of welding process using the AWI 6.13-2.
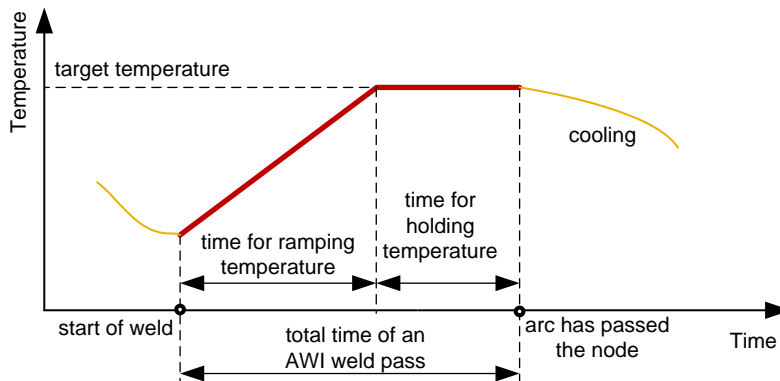
Figure 2. The prescribed temperature approach for nodes associated with a weld, modified from Lindgren (2001).

While the AWI procedure is quite straightforward, its accuracy can be expected to be highly dependent on user-defined inputs: magnitude of the torch temperature, specific values chosen for use in the temperature ramping option, and the deposited weld chunk length. To use the AWI capabilities, these parameters should be calibrated for a proper thermal solution to each welding simulation. The calibration can be difficult and expensive due to the lack of information about the effect of these modeling parameters, and the absence of guidance on the calibration procedure. In this paper, a sensitivity study based on the results of ten models will help close this gap in the literature. These models were created in Abaqus 6.13-3 using the AWI 6.13-2 utility with varying torch temperatures, ramping options, and deposited weld chunk lengths.

2.   Description of numerical analyses and calibration parameters

2.1   Model geometry

A research study performed by Peric et al. (2014) was selected as a benchmark study, as it included experimental data as well as a complete description of the utilized procedure for simulating the complete welding process.

As shown in Figure 3, two physical plates were welded to create a T-joint in the Peric et al. (2014) study. A welding current I = 270 A, arc voltage U = 29V, and welding speed v = 400 mm/min were used during the welding process. After placing the first fillet weld pass, the joint was cooled for a period of 215 s before the second weld was placed. The locations of the thermocouples are presented in Figure 3. In addition, temperature readings were also obtained using an SC2000 infrared camera.

The temperature field in the numerical portion of Peric et al.'s study was obtained by simulating the welding process using a distributed heat flux applied to the weld elements. The geometry and boundary conditions are presented in Figure 3.

2.2   Numerical model

Although the AWI is capable of generating both a thermal analysis and mechanical analysis, the scope of work presented in this paper is related to the former. A full description of the numerical steps used in the AWI modeling routine can be found in the AWI Users' Manual (Simulia, 2013).

For the sensitivity study that is the focus of this paper, a 3-D numerical model with temperature-dependent material properties and an elastic-plastic material model were used. The element types were the same as used in the study performed by Peric et al. (2014) (DC3D8 elements were applied for the thermal model, and C3D8 elements were applied for the mechanical stress analysis). Other modeling parameters, such as the Stefan-Boltzmann constant, $\sigma = 5.67 \times 10\text{-}8$ J/(m2K4), effective emissivity, $\varepsilon = 0.9$, convection heat transfer coefficient, hc = 10 W/m2/K, were also taken to be the same as used by Peric et al. (2014). Temperature-dependent thermal properties (Figure 4) and mechanical properties (Figure 5) were assumed to be the same for the weld and base metal (steel grade EN 10025-2: S355JR). The 3-D mesh used here included 24,600 elements (Figure 6), which should be expected to provide an adequate comparison with the results from Peric et al. (2014), which used 22,176 elements.
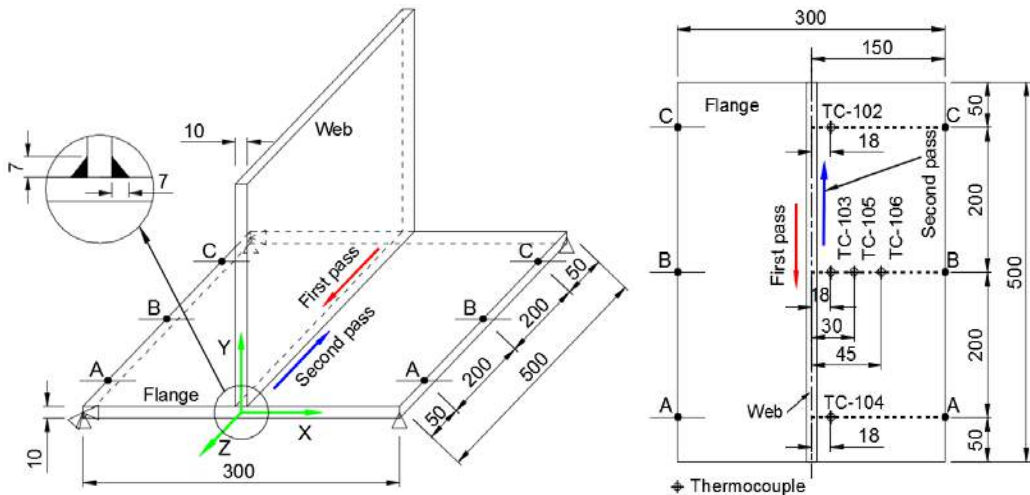

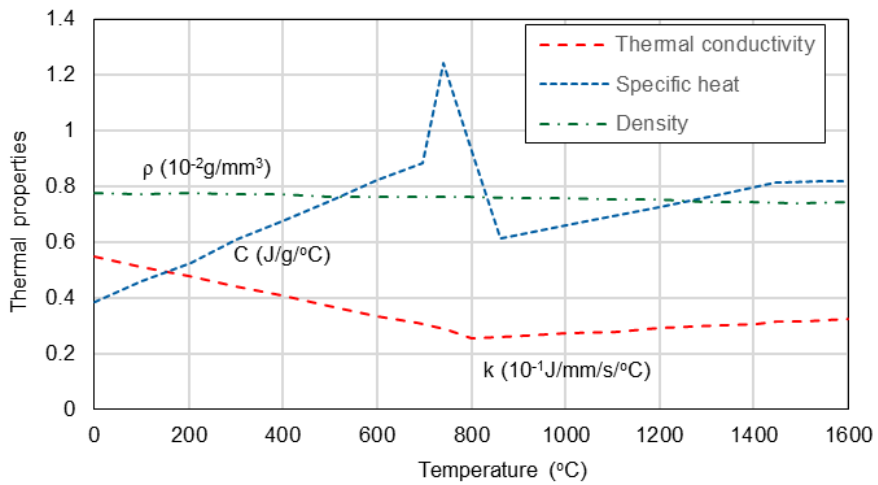**Figure 3. Weld geometry and thermocouple locations, adapted from Peric et al. (2014).**

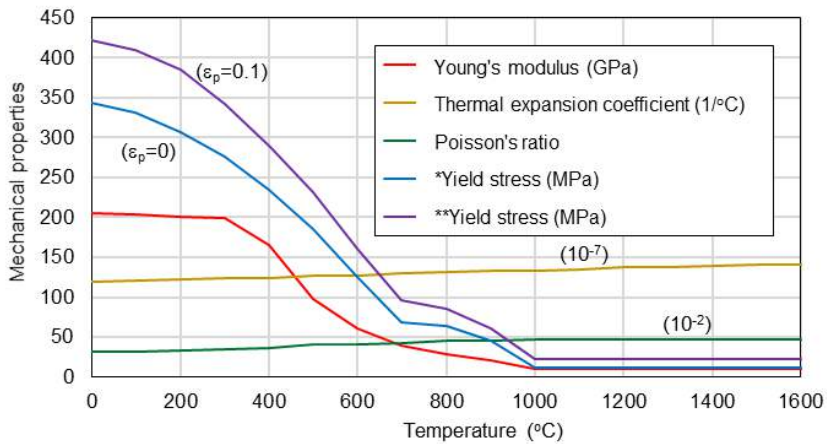**Figure 4. Thermal properties, adapted from Peric et al. (2014).**

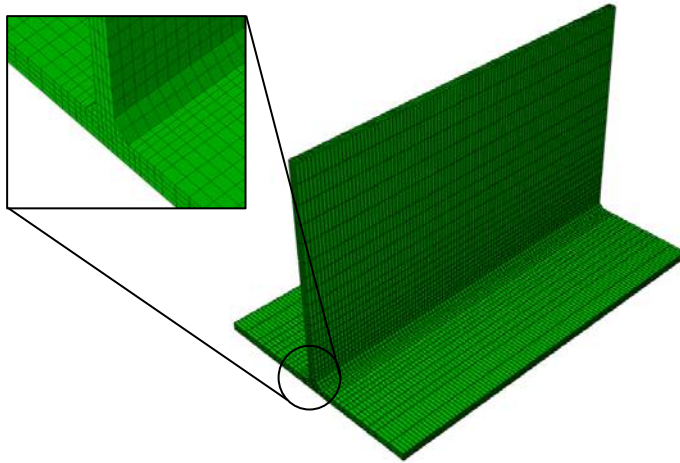**Figure 5. Mechanical properties, adapted from Peric et al. (2014).**

Figure 6. Finite element mesh for the models in the sensitivity study.

2.3   Calibration parameters

Three parameters must be calibrated in the AWI using the prescribed temperature approach to obtain a temperature field that accurately simulates the welding procedure from Peric et al. (2014):

- The first parameter included in this sensitivity study was the length of a weld chunk to be deposited into the weld pool over a specific period of time (called the *Time Period* in the AWI). In this study, four models having different deposited weld chunk lengths were chosen, as shown in Group 1 of Table 1. To define the Time Period in the AWI, the user need to calculate it based on the selected weld chunk length and the welding speed. In the work done by Peric et al., the welding speed was 400 mm/min. Therefore, for the case where a 10 mm deposited weld chunk length was desired, the step time was 10/6.667 = 1.5 s. As a result, a period of 1.5 s was input into the AWI to achieve a weld chunk length of 10 mm.

- The second parameter included in this study was the target torch temperature. Five models that included variations in torch temperature were used to examine the effects of this parameter, as shown in Group 2 of Table 1.

- The third parameter studied was the temperature ramping option. The temperature ramping values represent the time needed in term of a percentage of total AWI weld pass time (defined in Figure 2) to ramp the weld temperature to the target torch temperature. For example, for the case of 10% of a total pass time of 1.5 s, a period of 0.15 s would be used to ramp the current weld temperature from room temperature to the target torch temperature. Three models were chosen for this category, as shown in Group 3 in Table 1.

Table 1. Parameters of groups of models.

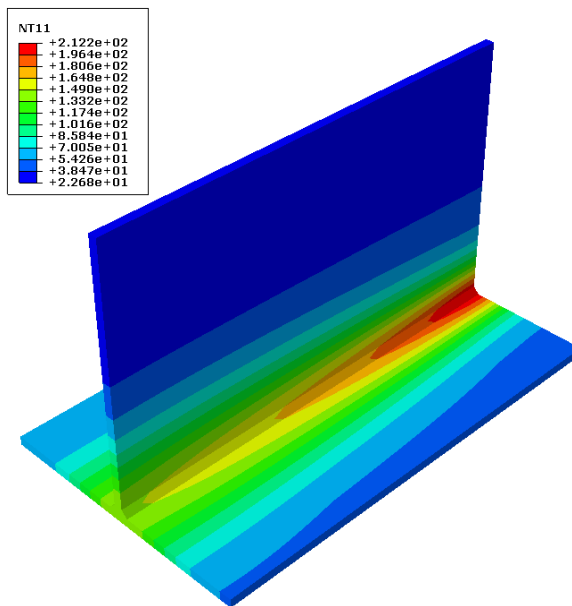| Varied Parameter	Model	Deposited weld chunk length (mm)	Target torch temperature (^{o}C)	Ramping option (%)
Group 1: Deposited weld chunk length	1	**50**	1500	10
	2	**20**	1500	10
	3	**10**	1500	10
	4	**05**	1500	10
Group 2: Target torch temperature	1	10	**1200**	10
	2	10	**1300**	10
	3	10	**1400**	10
	4	10	**1500**	10
	5	10	**1600**	10
Group 3: Ramping option	1	10	1500	**10**
	2	10	1500	**60**
	3	10	1500	**100**

Figure 7. Result of temperature distribution of model with parameters 1200 ^{o}C torch temperature, 10 mm weld chunk length, and 10% ramping option.

3. Results

Figure 7 shows the temperature distribution (at 403 s) obtained from the analysis of a model with the following parameters: torch temperature 1200 $^{\circ}$C, ramping option set at 10%, and a deposited weld chunk length of 10 mm. The results from Peric et al.'s study are also presented in Figure 7 as a comparison. It is observed that the obtained temperature field distribution in the model is in good agreement with Peric et al.'s finite element result. However, the main purpose of this paper is the sensitivity study of calibration parameters, which is presented as the following sections.

3.1   Deposited weld chunk length sensitivity

Figure 8 presents the temperature histories of four models with different deposited weld chunk lengths in comparison to the thermocouple measurement and numerical result from Peric et al.'s work. As seen in the figure, the larger the deposited weld chunk length, the greater the temperature generated. The temperature curve better mimics Peric et al.'s numerical results when smaller deposited weld chunk lengths are used. For example, at the location of thermocouple TC-102, the peak temperature is 417 $^{\circ}$C for the 50 mm weld chunk length case, while it is 290 $^{\circ}$C for the 5 mm weld chunk length case. Notice that the peak temperature of the thermocouple measurement was 260 $^{\circ}$C, and Peric et al.'s numerical result was 246 $^{\circ}$C. The similarity between the temperature histories for the cases of 10 mm and 05 mm weld chunk lengths shows a sign of convergence. Therefore, a weld chunk length of 10 mm was chosen for the following sensitivity studies. Figure 9 shows temperature profiles at lines A–A, B–B, and C–C, which are defined in Figure 3.
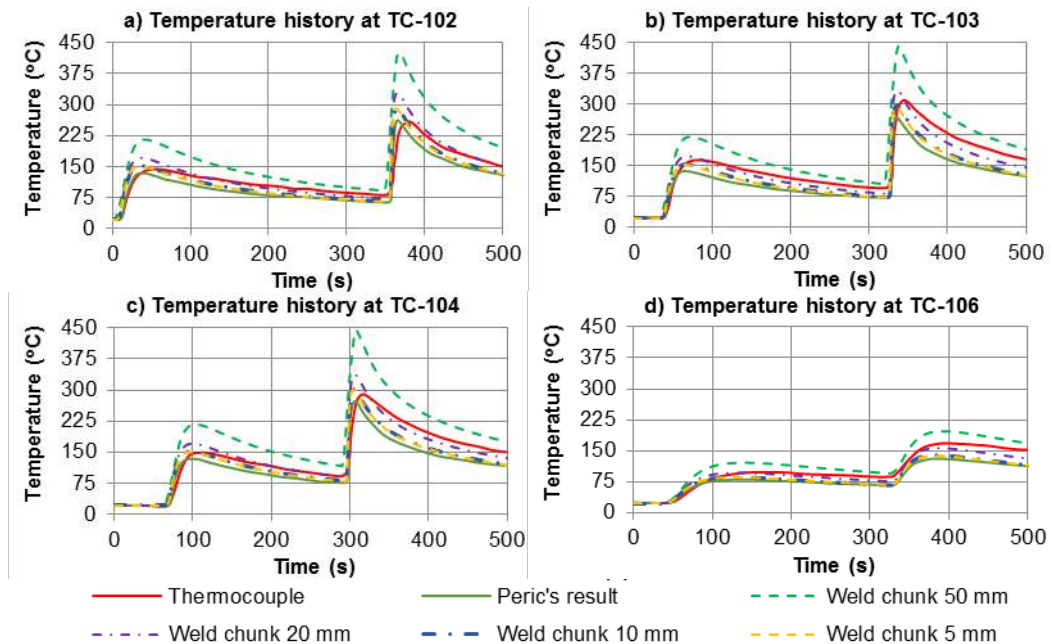

Figure 8. Temperature history at thermocouple locations produced by using different weld chunk lengths.
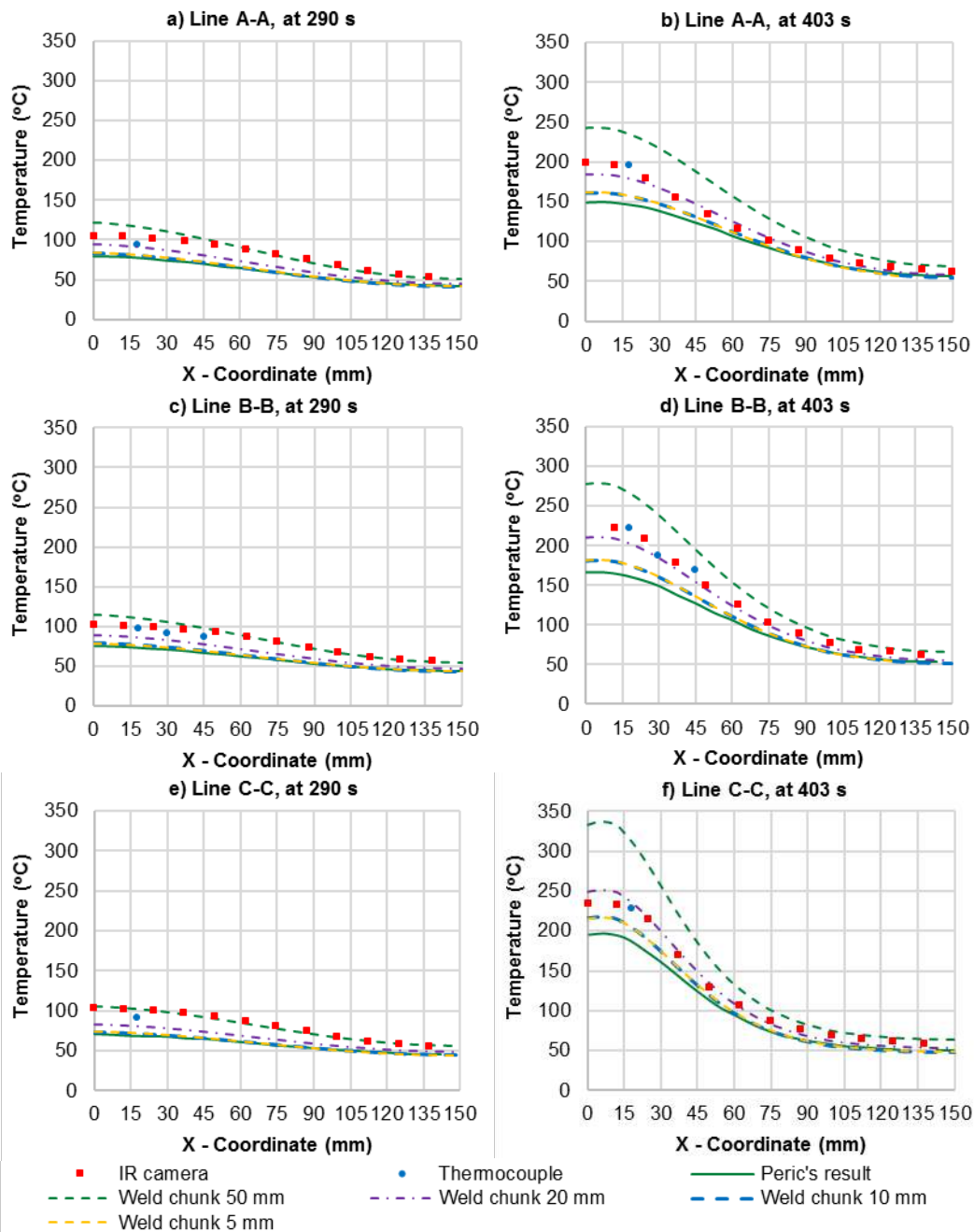
Figure 9. Temperature profiles produced by using different weld chunk lengths.
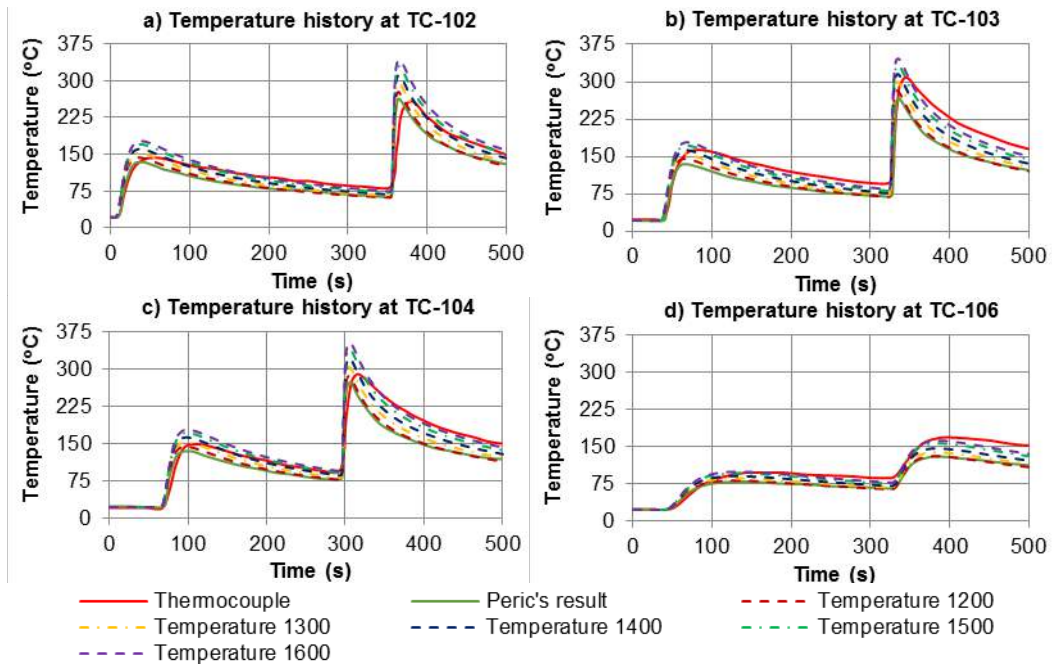
Figure 10. Temperature history at thermocouple locations produced by using different torch temperatures.

3.2   Torch temperature sensitivity

Figure 10 and Figure 11 present a comparison between predicted temperatures obtained using AWI with different torch temperatures and Peric et al.'s experimental and numerical results. As depicted, the torch temperature definition was found to have a strong effect on temperature history and temperature profiles in the model. Larger torch temperatures produce greater heat input, leading to temperature curves with higher peaks. However, it is non-trivial to determine which curve is optimal, as the peak temperature and the cooling curve tend to offset each other in terms of how well they approximate the experimental data. The models that included torch temperatures of 1400 ^{o}C and 1500°C seemed to generate the best-matched temperature predictions among the five models studied. It is worth acknowledging that the curves from the model that used a 1200 ^{o}C torch temperature are very close to the finite element result of Peric's work.

3.3   Ramping option sensitivity

Figure 12 and Figure 13 depict the results obtained when the ramping option was varied. Longer ramping times produce less heat input, leading to lower peak temperatures. The ramping option shows an effect on the temperature history, but resulted in less model sensitivity than varying the torch temperature. Therefore, it was found that the ramping option can be used as "fine-tuning" to obtain an improved result after torch temperature has been defined in a welding calibration using the AWI utility.
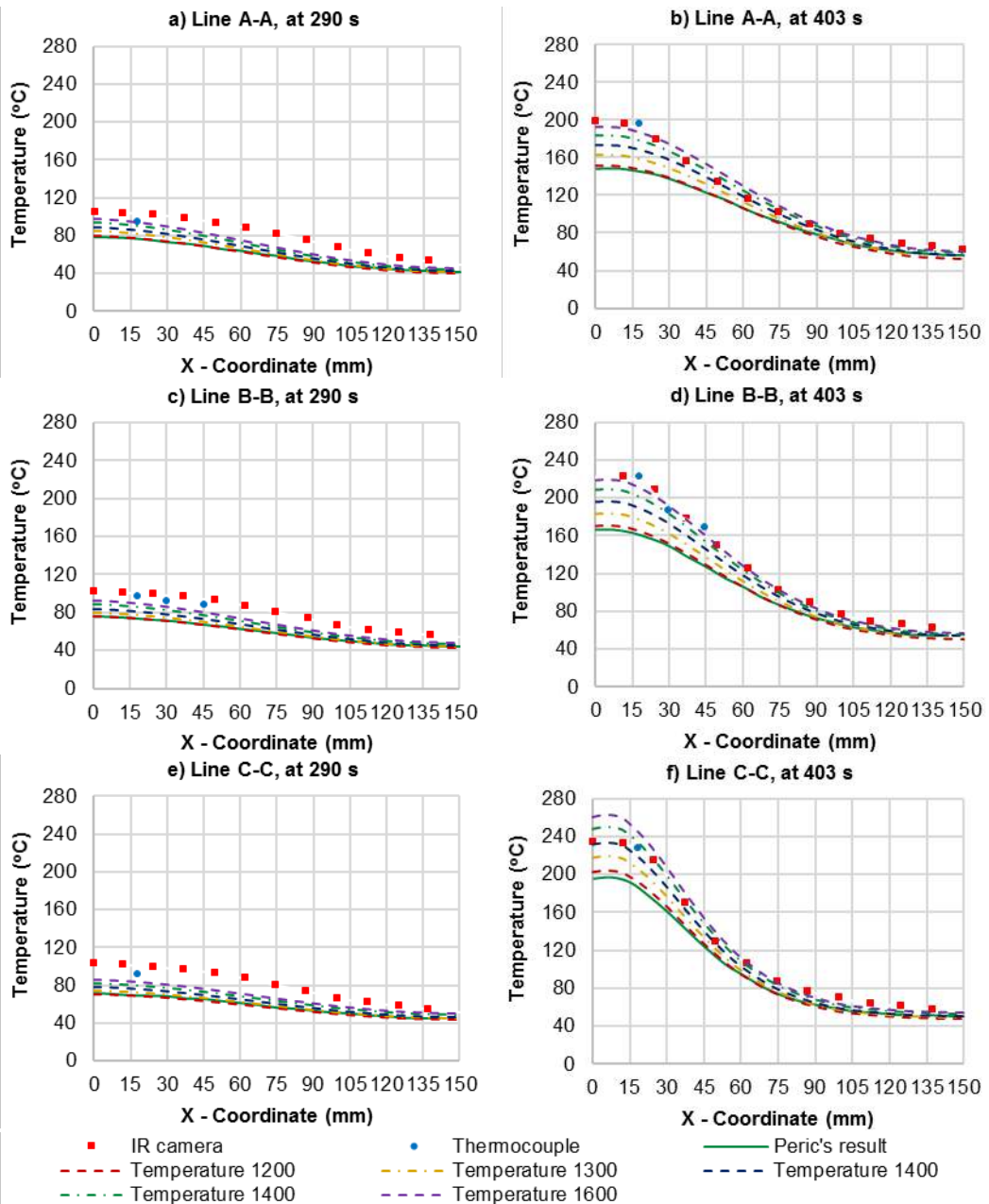
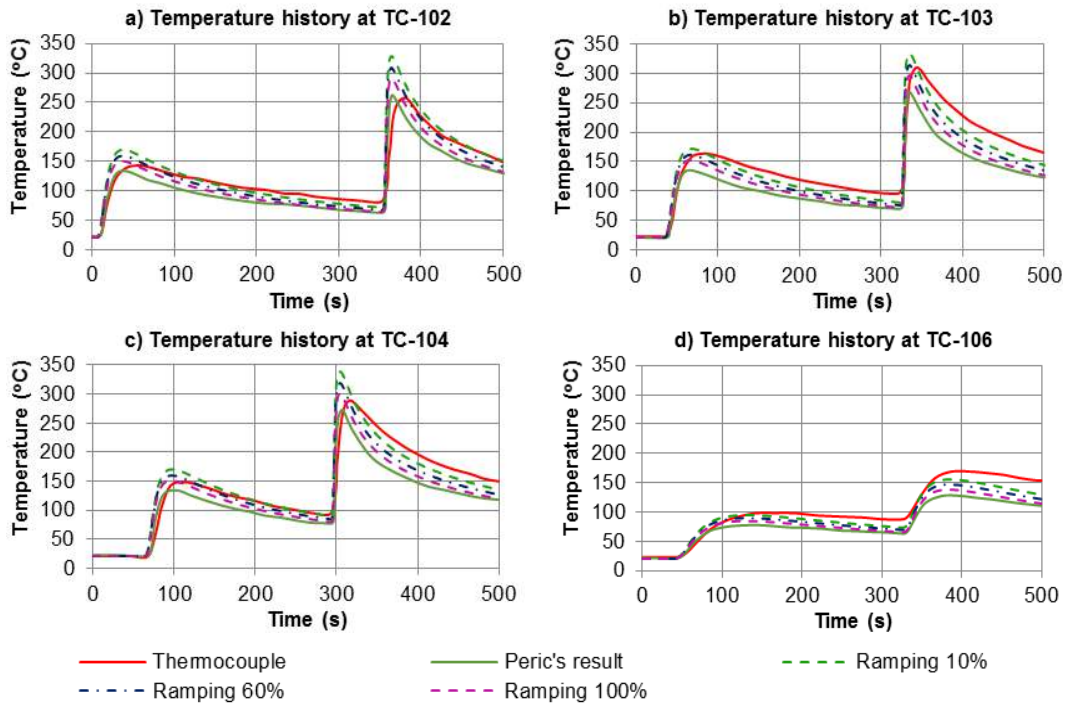**Figure 11. Temperature profiles produced by using different torch temperatures are studied.**

Figure 12. Temperature history at thermocouple locations produced by using different ramping options.
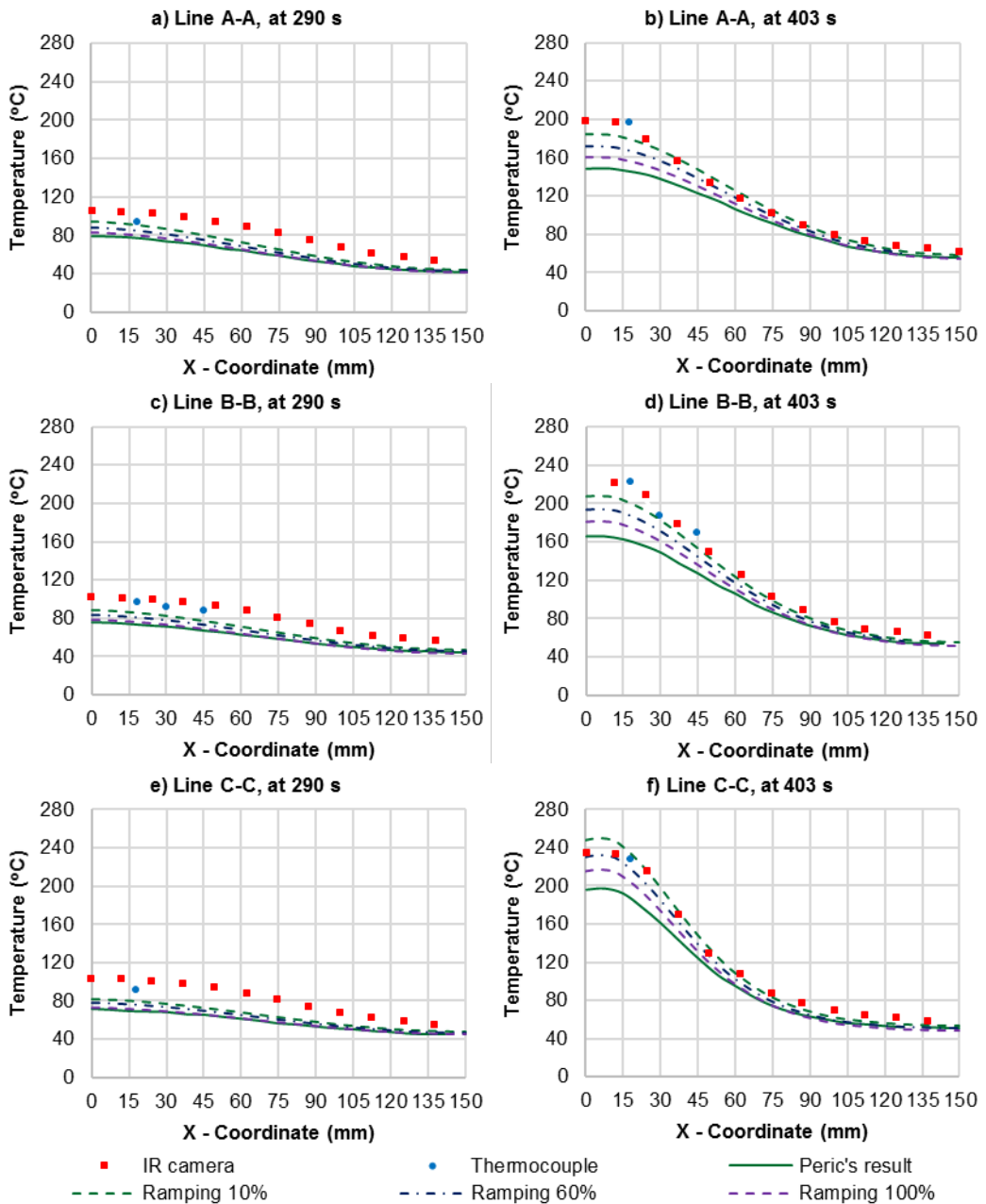
Figure 13. Temperature profiles produced by using different ramping options.

4. Discussion

4.1   Calibration of a welding simulation with prescribed temperature approach

Based on the results, it is known that the predicted temperature histories and profiles are sensitive to all three parameters studied: the deposited weld chunk length, the target torch temperature, and the selected ramping option. To calibrate a welding simulation, users of the AWI utility may need to select a set of parameters to generate the proper temperature field, in regard to matching experimental data. This task is made difficult by two conflicting objectives.

First, users should strive to select parameter inputs that reflect reality, such as using smaller weld chunk lengths and a small ramping option to depict the continuity of physically deposited weld metal and a torch temperature that is close to, yet above the melting temperature of the base metal, since the basis of welding relies on melting the joined materials.

Secondly, users should balance their implementation of actual welding parameters with numerical issues. For example, the smaller the deposited weld chunk length becomes, the more the number of steps for both thermal and mechanical analysis increase. A realistic torch temperature close to the melting temperature of 1500°C could generate an unreasonably high peak temperature. A ramping option that is in effect too steep can create convergence issues.

A recommended procedure for using the AWI utility with the prescribed temperature approach is as follows, arranged in order according to effect on predicted temperature history and profiles:

1. Study the influence of deposited weld chunk length to find convergence; select a weld chunk length that balances efficiency and convergence;

2. Choose the appropriate torch temperature that represents what was actually used in practice; and

3. Use the ramping option to make fine-tuning alterations to the results.

4.2   The merit of the AWI with prescribed temperature approach

The prescribed temperature approach used in the AWI utility was able to generate results that matched the finite element results produced by Peric et al. (2014), which relied on a distributed heat flux approach. Particularly, the AWI model that utilized a weld chunk length of 10 mm, torch temperature of 1200°C, and 10% ramping option predicted temperature histories and profiles which matched very well to the Peric et al.'s finite element results, as can be seen in Figure 10 and Figure 11. However, when the simulation results are compared to the experimental results, a lower level of agreement is observed. As seen in the temperature time histories in Figure 8, Figure 10, Figure 12, the peak temperatures were overestimated when torch temperatures in the range of 1300°C - 1600°C were used. They only reached the experimental results when a torch temperature of 1200°C, which was lower than that actually used, was selected.

The deviation between finite element and experimental peak temperatures noted in this study was also found to be a common thread in many published papers, such as work reported by Lindgren et al. (1999), Heinze et al. (2012); Kounde et al. (2012), and Keinanen (2016). As mentioned earlier, a welding simulation is a complex problem (Goldak & Akhlaghi, 2005; Lindgren, 2006). The results largely depend not only on the way in which the heat source is simulated, such as the

prescribed temperature approach used in this study, but also on the complexity of the geometry and the accuracy of the thermal properties, such as thermal conductivity, heat transfer convection coefficient and emissivity factor (Bendeich et al., 2009).

5. Conclusions

This paper has presented a sensitivity study of computer simulation of a T-joint fillet weld, examining three parameters that are used in the AWI utility. The three parameters studied were the deposited weld chunk length, target torch temperature, and the ramping option. Based on the findings of the study, a recommended procedure for calibrating a welding simulation using the AWI with the prescribed temperature was presented. These results are expected to be useful to users of the AWI utility as they calibrate numerical simulations against known welding parameters and experimental data.

6. References

Bendeich, P., Smith, M., Carr, D., & Edwards, L. (2009, July 26-30). *Sensitivity of Predicted Weld Residual Stresses in the Net Task Group 1 Single Bead on Plate Benchmark Problem to Finite Element Mesh Design and Heat Source Characteristics.* Paper presented at the ASME 2009 Pressure Vessels and Piping Division Conference, Prague, Czech Republic.

Carmet, A., Debiez, S., Devaux, J., Pont, D., & Leblond, J. B. (1988). *Experimental and numerical study of residual stresses and strains in an electron-beam-welded joint.* Paper presented at the 2nd International Conference on Residual Stresses (ICRS2), Nancy.

Goldak, J., & Akhlaghi, M. (2005). *Computational Welding Mechanics*: Springer.

Goldak, J., Chakravarti, A., & Bibby, M. (1984). New finite element model for welding heat sources. *Metallurgical transactions. B, Process metallurgy, 15*(2), 299-305.

Goldak, J., Zhou, J., Breidguine, V., & Montoya, F. (1996). Thermal stress analysis of welds: from melting point to room temperature. *Trans. JWRI, 25*(2), 185–189.

Heinze, C., Schwenk, C., & Rethmeier, M. (2012). Numerical calculation of residual stress development of multi-pass gas metal arc welding. *Journal of Constructional Steel Research, 72*, 12 -16.

Jones, B., Emery, A., & Marburger, J. (1993a). An analytical and experimental study of the effects of welding parameters in fusion welds. *Welding Journal, 72*(2), 51–59.

Jones, B., Emery, A., & Marburger, J. (1993b). Design and analysis of test coupon for fusion welding. *ASME Journal of Pressure Vessel Technology, 115*, 38–46.

Keinanen, H. (2016). Computation of residual stresses for a repair weld case. *Welding in the World, 60*(3), 507-513.

Kounde, L., Engel, T., Bergheau, J.-M., & Boisselier, D. (2012). Thermo-mechanical Modeling of Laser-MAG Hybrid Welding and Consequences on Large Structure. *Materials Performance and Characterization, 1*(1), 1-17.

Lindgren, L.-E. (2001). Finite Element Modeling and Simulation of Welding Part 1: Increased Complexity. *Journal of Thermal Stresses, 24*, 141-192.

Lindgren, L.-E. (2006). Numerical modelling of welding. *Computer methods in applied mechanics and engineering, 195*, 6710–6736.

Lindgren, L.-E., Runnemalm, H., & Nasstrom, M. O. (1999). Simulation of multipass welding of a thick plate. *International Journal for Numerical Methods in Engineering, 44*(9), 1301–1316.

Peric, M., Tonkovic, Z., Rodic, A., Surjak, M., Garasic, I., Boras, I., & Svaic, S. (2014). Numerical analysis and experimental investigation of welding residual stresses and distortions in a T-joint fillet weld. *Materials and Design, 53*(12), 1052–1063.

Roelens, J.-B. (1995a). *Determination of residual stresses in submerged arc multi-pass welds by means of numerical simulation and comparisons with experimental measurements*. Paper presented at the Mathematical Modelling of Weld Phenomena, Graz University of Technology.

Roelens, J.-B. (1995b). Numerical simulation of multipass submerged arc welding—determination of residual stresses and comparison with experimental measurements. *Welding World, 35*(2), 110–117.

Roelens, J.-B., Maltrud, F., & Lu, J. (1994). Determination of residual stresses in submerged arc multi-pass welds by means of numerical simulation and comparison with experimental measurements. *Welding World, 33*(3), 152–159.

Shubert, M., Pandheeradi, M., Arnold, F., & Habura, C. (2010). *An Abaqus Extension for Welding Simulations*. Paper presented at the 2010 SIMULIA Customer Conference, Providence, Rhode Island, USA.

Simulia. (2013). Abaqus Welding Interface (AWI) - User's Manual.